



Time-dependent search for neutrino multiflare sources with the IceCube 59-string data

THE ICECUBE COLLABORATION¹

¹See special section in these proceedings

Abstract: A time-dependent search for neutrino flares from pre-defined directions in the whole sky is presented. The analysis uses a time-clustering algorithm combined with an unbinned maximum likelihood method. This algorithm, by including a likelihood signal term describing the contribution of many small clusters of signal-like events, provides an effective way for looking for weak neutrino flares over different time-scales. The event selection is optimized to maximize the discovery potential for the IceCube 59-string (IC59) detector configuration. Sources are being selected based on data in the 0.1 to 100 GeV energy range as provided by the Fermi satellite. Subsequently, periods of interest based on electromagnetic data are scanned, over larger time-windows as compared to the duration of the corresponding electromagnetic flares.

Corresponding authors: Dariusz Góra^{2,3} (Dariusz.Gora@desy.de), Elisa Bernardini² (Elisa.Bernardini@desy.de), Angel Cruz Silva² (angelh@ifh.de)

DOI: 10.7529/ICRC2011/V09/0289

² DESY, D-15738 Zeuthen, Germany

³ Institute of Nuclear Physics PAN, Radzikowskiego 152, 31-342 Cracow, Poland

Keywords: IceCube; Neutrino Flares; Time-dependent searches

1 Introduction

Finding neutrino point sources in the sky requires locating an excess of events from a particular direction over the background of atmospheric neutrinos and muons. Signal events might present additional features that distinguish them from background, for example a different energy spectrum or time structure. For sources which manifest large time variations in the emitted electromagnetic radiation, the signal-to-noise ratio can be increased by testing smaller time windows around the flare (time-dependent search). Following this idea there are in principle two approaches to neutrino time-dependent searches: Triggered and Untriggered. In the first case we are looking directly for photon-neutrino correlations using specific source lightcurves from Multi-WaveLength (MWL) observations [1]. In the second case, followed in this work, we perform a generalized search for neutrino flares from a pre-selected source list, motivated by (but not directly in time coincidence with) MWL observations. This approach allows to account for possible time lags between photon flares and the associated neutrino flares [2].

An untriggered unbinned flare search was first developed and applied to IceCube data, using a compact list of pre-defined source directions [3]. IceCube is km³ scale neutrino detector at the South Pole sensitive to TeV-neutrinos [4]. A time-clustering algorithm [3, 5], and an unbinned maximum likelihood method [6] are the basis of

this analysis. Such a method finds the most significant flare in a long period. The number of trials coming from all combinations of event times is increased, reducing the significance. However, for flares sufficiently shorter than the total observation period, the time clustering algorithm is more sensitive than a time-integrated analysis.

In this paper, we propose an extension of the method described in [3]. The proposed algorithm can extract not only the most significant flare, but also less significant clusters of events distributed over several weak flares. These weaker flares could have any separation in time and therefore may be very difficult to detect or even undetectable with other existing point-sources methods (like [6]).

2 Multiple flare search algorithm

A more detailed description of the proposed method and its application for multi-flare Monte Carlo simulation can be found in [7]. Here we only briefly describe the main steps of the proposed algorithm. In order to identify a series of weak flares, we first extract all *consecutive* doublets that can be formed out of all signal-like events ($S_i/B_i > 1$) over the data taking period ΔT_{data} ¹, see Figure 1.

1. A signal-like event is defined as having $S_i/B_i > 1$, where S_i and B_i are the signal and background Probability Density Function (PDF), respectively, as defined for the time-integrated

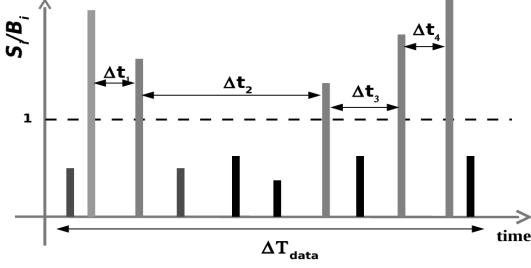


Figure 1: The basic idea of the time-clustering procedure.

This step serves to isolate all possible (and smallest) time windows (Δt_j) that compose the signal contribution in the tested data sample (the total number being M). We call these time windows “data segments”. Note, that by using only doublets as data segments we do not need any assumptions about the distribution of signal events inside a data segment i.e. by definition the time probability P^{time} in the signal PDF is uniform in time and is given by $P^{\text{time}} = \frac{1}{\Delta t_j}$.

Then for each data segment the best estimates of the number of signal events \hat{n}_s and source spectral index $\hat{\gamma}_s$ are found by maximizing the one-source likelihood as defined in [6]. Then for each data segment the individual value of the test statistic $\text{TS}_j|_{\Delta t_j}$ is calculated from the likelihood ratio of the background-only (null) hypothesis over the signal-plus-background hypothesis [6]. All data segments are then sorted according to $\text{TS}_j|_{\Delta t_j}$. In the case that real signal events are present, some of these data segments will contain the signal events while the rest of them are due to background fluctuations. Our aim is to extract the optimal (best suited) number of data segments (M_{opt}) which compose the total signal contribution in the overall period ΔT_{data} .

For this purpose, we used a modification of the single-source likelihood function ([6]) by replacing the one-source signal term S_i by the sum of signal sub-terms over m data-segments:

$$S_i \rightarrow \frac{\sum_{j=1}^m W^j \times S_i^j(|\vec{x}_i - \vec{x}_s|, E_i, \gamma, \Delta t_j)}{\sum_{j=1}^m W^j} \quad (1)$$

where W^j is a weight which describes the strength (significance) of the doublet contained in each data segment. As was shown in [7] the test statistic is quite well correlated with the true number of injected signal events. Thus we take $W^j = \text{TS}_j|_{\Delta t_j}$.

In order to estimate the optimal number of data segments M_{opt} for a given configuration of m segments (starting from $m = 1$) we maximize the modified $\log(\tilde{\mathcal{L}}(n_s, \gamma_s, m))$ with n_s and γ_s as free parameters. For a given number m the minimization returns the best estimates for the number of signal events \hat{n}_s and for the spectral index of the source $\hat{\gamma}_s$, and the “global” test statistic is calculated from:

$$\tilde{\text{TS}}(m) \equiv -2 \log \left[\frac{\tilde{\mathcal{L}}(\vec{x}_s, n_s = 0)}{\tilde{\mathcal{L}}(\vec{x}_s, \hat{n}_s, \hat{\gamma}_s, m)} \right]. \quad (2)$$

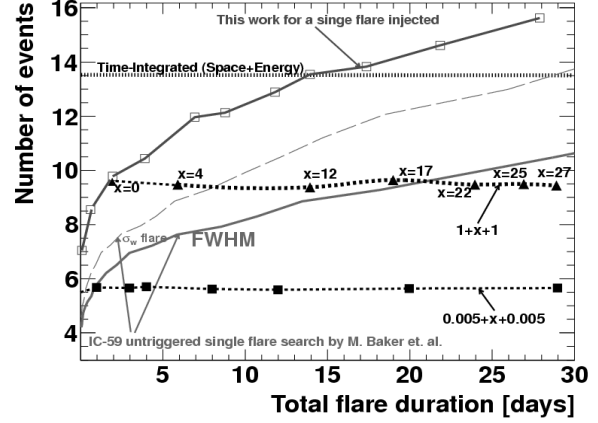


Figure 2: Number of events for a 5σ discovery as a function of the total flare duration obtained for one flare search and two flares search. See text for more details.

Then, the optimal number of data segments to be stacked (M_{opt}) is chosen according to the maximum of $\tilde{\text{TS}}(m)$. The overall significance of the optimal configuration M_{opt} can be determined using MC simulations by applying the same procedure to a large number of scrambled data sets.

3 Data Sample

IceCube 59-string data from May 20, 2009 to May 31, 2010 is used. It spans 375 days with an overall effective detector uptime of 93% (i.e. 348 days). The whole sky (declination range from -85° to 85°) is scanned. Different selection criteria, due to different backgrounds, are applied for the northern and southern skies, see [8]. After selection the data set contains 107 569 events (43 339 events in the northern sky and 64 230 events in the southern sky) with a median angular resolution of 0.7° .

4 Expectations for IceCube 59-strings

Figure 2 shows the performance of the algorithm for a source with a E^{-2} energy spectrum located at declination $\delta = 22^\circ$. For a single flare search (solid line with open boxes) the number of events for a 5σ discovery decreases when we consider flares with shorter duration. As an example, for a flare with duration of 28, 10 and 0.1 days in average about 15, 12 and 7 events, respectively, are needed for discovery. Note, that for flares with relatively short durations (below about 15 days) the number of events is smaller compared to a time-integrated analysis, see dashed line in Figure 2 labeled: Time Integrated Analysis (Space+Energy). In Figure 2 the performance of the algorithm for two flare searches is also shown (horizontal dashed lines).

In this case two individual flares with duration $\Delta t_{\text{flare}}^{(1)}$ and $\Delta t_{\text{flare}}^{(2)}$, respectively, are separated in time by a time interval Δt_{flare} . To calculate the ratio, $S_i/B_i > 1$, only the spatial and energy terms in the PDF’s are included.

terval x .² For two flares separated by x we can see that the number of events needed for discovery only slightly depends on the total flare duration $\Delta T(M_{opt})$ and equals the case of single flare with duration ($\Delta T(M_{opt}) = \Delta t_{flare}^{(1)} + \Delta t_{flare}^{(2)}$) i.e. $x = 0$. This is a consequence of the fact that the proposed algorithm looks for the total signal in the data sample but disregards how these signal events are distributed in time. In other words, signal events form in time one significant cluster of events (one flare) for a given source location, or these events can be distributed among a few (sometimes less significant) flares separated in time. Figure 2 shows also that multiple flares have better discovery potential than that of one flare if the same method is used.

For comparison purposes, in Figure 2 the performance of an untriggered time-dependent analysis from [8] is shown. In this case calculations are performed using the standard unbinned likelihood method with the assumptions, that the shape of the flare follows the Gaussian distribution i.e. so called Gaussian burst [6]³. Comparing our results for a single flare with [8] we need about 50% more events for discovery in case all events are injected in one single flare. This is because our algorithm stacks also background fluctuations, and thus leads to a higher 5σ threshold than the threshold obtained by a single-source likelihood based method. However, if we consider two flares separated in time the differences in the number of events strongly decreases and with enough separation in time the multi-flare analysis requires fewer events for discovery than standard untriggered searches. As an example for two flares 1 day long each, if they are separated by more than 20 days, the multi-flare search performs better than [8]. A similar behavior is observed for individual flares with duration $\Delta t_{flare}^{(1)} = 0.005$ day, i.e. for time scales of the order of minutes.

In Figure 3 the fluence sensitivity for IceCube 59-string data is presented for six representative source directions. The fluence depends on the total data period ΔT_{data} considered, being better for smaller data periods. The fluence increases when we consider flares with longer duration. The effect is well visible for $\Delta T_{data} = 40$ days.

5 Source selection and results

The proposed algorithm was applied to selected sources which manifest large time variations in the electromagnetic flux. Using our multiple search algorithm we do not need a precise estimation of the starting time and ending time of each flare. As was shown in [7] the algorithm finds all signal events in the data period even if signal events are arranged as a few clusters separated in time. Thus we only need a first guess of the flare central time T_m and we set a larger time window: $T_m \pm 40$ days. This allows to search for neutrino flares near a γ , optical, x-ray or infra-red flare testing the correlation or anticorrelation in the neutrino-gamma emission.

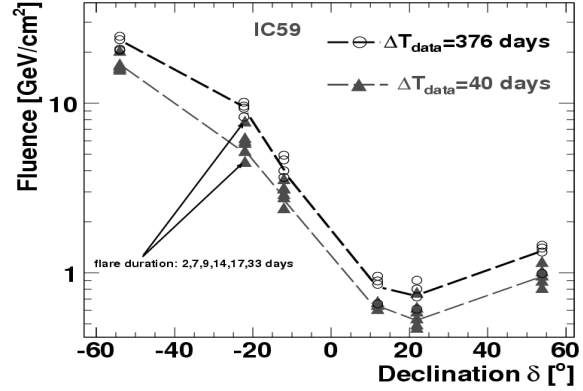


Figure 3: Fluence sensitivity from an E^{-2} spectrum neutrino signal plotted versus declination for different observation times using IceCube 59-string data.

In the context of hadronic models predicting high energy neutrino emission from objects such as Active Galactic Nuclei (AGN), there are several possible scenarios. For example in [2] Flat Spectrum Radio Quasars (FSRQ) are more promising, as neutrino sources, than BL-Lac objects, whereas in [9] the opposite is predicted. The proton blazar model [10] predicts that the Low synchrotron peaked BL-Lacs (LBL) are more likely to produce a significant neutrino emission than the High synchrotron peaked BL-Lacs (HBL). In [9] harder sources are selected as promising sources to be detected by IceCube once the prediction of the neutrino fluxes, within the assumed pp model, is combined with the IceCube instrumental response. On the other hand in [2] the considered $p\gamma$ model leads to the conclusion that FSRQs bright in the GeV range are promising neutrino sources without any assumption on the spectral index. In order to include these different predictions in this analysis data from the first Fermi LAT catalog [14] was used to select AGNs according to the following criteria:

- **BL-Lacs:** Average flux [1 – 100 GeV] $> 1 \times 10^{-9}$ ph $\text{cm}^{-2}\text{s}^{-1}$ AND Spectral index < 2.3
- **FSRQs:** Average flux [0.1 – 1 GeV] $> 7 \times 10^{-8}$ ph $\text{cm}^{-2}\text{s}^{-1}$

In addition for both cases we include a variability index cut ($V > 23.21$) to select sources that are more likely to exhibit flaring periods [14]. For the selected sources, information about flaring states in different wavelengths, during the period of the 59-string configuration of IceCube was collected. The selected sources and periods are presented in Table 1.

2. In this case the total flare duration is defined as $\Delta T(M_{opt}) \equiv \Delta t_{flare}^{(1)} + x + \Delta t_{flare}^{(2)}$, so for example configuration $1 + x + 1$ corresponds to two one day flare each separated by time interval x ranging from 0 up to 27 days.

3. In this work simulated signal events are injected according to a uniform time distribution, while in [8] a Gaussian distribution with different standard deviation σ_w was considered. To make comparison, the corresponding width at half maximum $FWHM = 2\sqrt{2 \ln 2} \sigma_w$ is calculated for a Gaussian flare, and then these results are compared with our calculations.

Table 1: Results for pre-defined variable astrophysical source candidates using the multi-flare algorithm.

Source	Type	ra [deg]	dec [deg]	#Atel / ref	T_m^* (MJD)	p-value	$\Delta T(M_{opt})$ [days]	Fluence Limit [GeV/cm ²]
PKS 0235+164	LBL	39.67	16.62	2207 / [11]	55085	0.27	0.0060	0.54
Mkn 421	HBL	166.12	38.21	2368 / [12] 2443 / [12]	55200 55255	1.0 0.34	4.11 0.13	0.90 0.73
PKS 0426-380	LBL	67.16	-37.94	2366	55198	1.0	14.41	14.3
PKS 0537-441	LBL	84.72	-44.08	2124 2454 2591	55020 55247.5 55313	0.45 1.0 1.0	7.21 25.68 1.18	15.7 17.44 15.2
S5 0716+714	LBL	110.48	71.34	2353	55176.5	0.34	3.90	1.30
PKS 0447-439	HBL	72.38	-43.84	2350	55180	1.0	4.80	15.5
PKS 1424+240	HBL	216.75	23.8	2098	54977	1.0	0.44	0.59
PKS 0301-243	IBL	45.89	-24.11	2610	55319	0.36	0.775	7.37
3C 454.3	FSRQ	343.49	16.15	2534 2329 / [11] 2200 / [11]	55289 55167 55089	1.0 0.22 0.08	1.84 0.045 28.67	0.64 0.52 0.86
3C 279	FSRQ	194.05	-5.79	2154	55044	1.0	1.10	1.40
PKS 2023-07	FSRQ	306.42	-7.6	2175	55066	1.0	0.81	1.80
3C 273	FSRQ	187.28	2.05	2200 / [13] 2376	55089 55203	1.0 1.0	0.365 1.28	0.71 0.81
4C +31.03	FSRQ	18.23	32.12	2054	54971	1.0	1.43	0.68
PKS 0805-07	FSRQ	122.05	-7.84	2136 2048	55034 54958	1.0 1.0	3.85 10.34	2.03 1.91
PKS 0402-362	FSRQ	60.98	-36.06	2484	55228	1.0	13.17	12.88
B2 1520+31	FSRQ	230.55	31.73	2026	54941	1.0	4.85	0.65
OX 169 325.87	FSRQ	325.87	17.72	2393	55214	1.0	1.54	0.64
PKS 2052-47	FSRQ	314.09	-47.24	2160	55052	1.0	0.62	15.36
4C +38.41	FSRQ	248.77	38.14	2456 2136	55250 55034	1.0 0.17	3.17 0.023	0.81 0.69
PKS 0906+01	FSRQ	137.27	1.44	2543	55294	0.16	0.154	0.71
PKS 0420-01	FSRQ	65.	-1.31	2402	55217	0.59	1.1	0.96
PKS 1830-21	FSRQ	278.41	-21.06	2242	55116.5	1.0	1.92	6.67
PKS 0244-470	FSRQ	41.5	-46.87	2440	55239	1.0	12.92	17.96

* T_m is the midpoint of the flare time interval reported in the alert (Atel) or in the corresponding reference when available.

$\Delta T(M_{opt})$ is the flare duration calculated for the optimal configuration of M_{opt} data segments.

The fluence upper limit is calculated by integrating $d\Phi/dE \times E$ over the 90% energy range and $\Delta T(M_{opt})$, assuming a neutrino energy spectrum of E^{-2} .

The proposed method was applied to the selected source candidates. No significant excess above the atmospheric background is found, therefore upper limits on the neutrino fluence were calculated. The results are presented in Table 1. The highest fluctuation observed corresponds to 3C 454.3 with a p-value of 8% (not including the trial factors due to looking at several sources). The limits for IC59 are on average about 50% better than for IceCube 40-strings data [15].

6 Summary

We presented a method to search for neutrino flares from point sources without an *a-priori* assumed time structure. The method considers only data segments which contain signal-like doublets, and uses a test-statistic term as their weights in a stacking-like calculation for the global maximum likelihood. For flares sufficiently shorter than the total observation period, the method is more sensitive than a time-integrated analysis and in some cases is also more sensitive than single flare searches already in use (like [8]). IceCube 59-string data was analyzed using the proposed method looking for neutrino multi-flares with no *a-priori* assumption on the time structure of the signal. A list of promising source candidates was selected based on

different hadronic models. Since no deviation from the background-only hypothesis was found, upper limits on the neutrino fluence from these sources were derived.

References

- [1] M. Baker et al., for the IceCube Collab., the 31st ICRC, Lodz, Poland, July 7-15, 2009 .
- [2] A. Atoyan et al., *New Astron. Rev.*, 2004, **48**: 381.
- [3] J.L. Bazo Alba et al, arXiv:0908.4209.
- [4] H. Kolanoski, IceCube summary talk, these proceedings.
- [5] K. Satalecka et al; arXiv:0711.0353.
- [6] J. Braun et al., *Astropart. Phys.* (2008) **29**: 299-305; J. Braun et al., *Astropart. Phys.*, 2010, **33**:175-181.
- [7] D. Góra et al., *Astropart. Phys.* (2011) **35**: 201-210.
- [8] IceCube Collab., paper 0784, these proceedings.
- [9] A. Neronov et al., *Phys. Rev. D*, 2009, **80**: 083008.
- [10] A. Mücke et al., *Astropart. Phys.*, 2003, **18**: 593-613.
- [11] R. Chatterjee et al., arXiv:1101.3815.
- [12] N. Isobe et al., arXiv:1010.1003.
- [13] A.A. Abdo et al., *Astro. J. Lett.*, 2003, **714**: 615-627.
- [14] A.A. Abdo et al., *Astro. J. Supp.*, 2010, **188**: 405-436.
- [15] The IceCube Collaboration; arXiv:1104.0075v1.